Journal of Radioanalytical and Nuclear Chemistry
https://doi.org/10.1007/s10967-024-09633-0

Synthesis and preclinical evaluation of [^{18}F]AlF-NOTA-Glc-Folate as a novel folate-receptor-targeted PET tracer

Haoran Liang[1,2] · Zihao Chen[1,2] · Shuqi Ren[1] · Chunwei Mo[1] · Ganghua Tang[1,2]

Received: 12 February 2024 / Accepted: 18 June 2024

Abstract
A novel ^{18}F-labeled radiotracer ([^{18}F]AlF-NOTA-Glc-Folate) modified with a hydrophilic linker (-Glc-) was developed for PET imaging of folate-receptor-positive tumors. [^{18}F]AlF-NOTA-Glc-Folate was manually synthesized within 30 min with high radiochemical yield and radiochemical purity. Cellular studies exhibited that [^{18}F]AlF-NOTA-Glc-Folate had a high specificity and affinity for the folate-receptor. Biodistribution and micro-PET imaging results showed proper uptake of [^{18}F]AlF-NOTA-Glc-Folate in tumors, as well as low uptake and rapid clearance in most normal organs, except for the kidney. [^{18}F]AlF-NOTA-Glc-Folate seems to be a potential radiotracer for PET imaging of tumors with folate-receptor expression.

Keywords [^{18}F]AlF-NOTA-Glc-Folate · Folate receptor-α · Micro-PET imaging · Pharmacokinetic property

Introduction

Folate receptor (FR) is a membrane-bound protein with a high affinity for physiological folic acid, even at low nanomolar concentrations [1]. There are several subtypes of FR, including FR-α, FR-β, FR-γ, and FR-δ. Among these, FR-α stands out as a promising target for tumor imaging due to its overexpression in a variety of epithelial tumors, such as lung, breast, ovarian, endometrial, and colorectal cancers, and it is weakly expressed in normal organs, except for the kidney. In addition, FR-α is involved in the accumulation of cellular folate through receptor-mediated endocytosis [1–3]. Given its potential applications in identifying and treating FR-positive tumors, FR has been an intriguing target for the diagnosis and treatment of tumors with folate receptor overexpression.

Numerous positron emission tomography (PET) imaging tracers based on FR have been developed for the diagnosis of FR-expressing tumors [4–15]. Nevertheless, except for a few tracers, such as [^{18}F]-AzaFol [8], ^{111}In-DTPA-Folate [9] and ^{99m}Tc-EC20 [10], the majority of these tracers fail to meet the stringent requirements for clinical translation due to complex labelling procedures, low product purity, or high uptake in non-target organs. The radiolabeling technology with "[^{18}F]AlF" has been applied successfully in research and has enabled convenient labeling of folate derivative tracers with [^{18}F]F$^-$. In 2016, Chen et al. [16] synthesized [^{18}F]AlF-NOTA-Folate via a one-step reaction of aluminum fluoride chelation, and biodistribution studies showed that [^{18}F]AlF-NOTA-Folate was highly specific bound to FR positive KB tumors [10.9 ± 2.7% ID/g, 90 min post-injection (p.i.)]. However, [^{18}F]AlF-NOTA-Folate was not optimal in kidney and liver (kidney: 78.6 ± 5.1% ID/g; liver: 5.3 ± 0.5% ID/g, 90 min p.i.). To circumvent the high uptake of folate derivative tracers by the kidney and the hepatobiliary system, the same group [14] later introduced the PEG_{12} group on the basis of [^{18}F]AlF-NOTA-Folate to increase its hydrophilicity. Compared with [^{18}F]AlF-NOTA-Folate, [^{18}F]AlF-NOTA-PEG_{12}-Folate improved uptake in kidney and liver (kidney: 55.2 ± 7.4% ID/g; liver: 1.6 ± 0.3% ID/g, 90 min p.i.), indicating that increased hydrophilicity led to improved pharmacokinetic behavior of PEGylated folate derivatives, however [^{18}F]AlF-NOTA-PEG_{12}-Folate showed decreased tumor uptake and high renal uptake. Suboptimal in vivo pharmacokinetics, especially the high uptake in the kidney and hepatobiliary system, is an important limiting factor for the clinical translation of most FR-based radiotracers

✉ Ganghua Tang
gtang0224@smu.edu.cn

[1] GDMPA Key Laboratory for Quality Control and Evaluation of Radiopharmaceuticals, PET Center and Department of Nuclear Medicine, Nanfang Hospital, Southern Medical University, Guangzhou 510515, China

[2] School of Pharmaceutical Sciences, Southern Medical University, Guangzhou 510515, China

Published online: 11 July 2024

[11–13]. To meet the stringent requirements for clinical translation, it is necessary to improve its pharmacokinetic properties by modifying the structure of the folic acid.

Our previous studies showed that the introduction of hydrophilic linker like Glc(-2-acetamido-2-deoxy-β-D-glucosylamine) into a radiotracer could increase hydrophilicity and reduce hepatobiliary metabolism [17]. In addition, Glc has been widely used to improve the in vivo clearance characteristics and facilitate the optimization of active drug delivery of radiotracers [18–21]. In this study, we introduced a Glc linker between the chelator NOTA(1,4,7-triazacyclononane-1,4,7-triacetic acid) and the pharmacophore FR-specific ligand to develop a folic acid derivative PET tracer ([^{18}F]AlF-NOTA-Glc-Folate) via Al^{18}F-chelation one-step reaction. Furthermore, a comprehensive preclinical assessment was performed on [^{18}F]AlF-NOTA-Glc-Folate with FR-positive KB cells and FR-negative A549 cells, including its stability, affinity for FR, cellular characteristics, biodistribution patterns, and imaging properties.

Materials and methods

General

All of the reagents were commercially purchased, of analytical grade, and utilized without further purification. NOTA-Glc-Folate was purchased from Nanchang TanzhenBio Co., Ltd. (Nanchang, China), with high chemical purity (> 95%). Folic acid (Sigma-Aldrich, P8798-5G) was acquired from Guangzhou Lusheng Technology Co., Ltd. (Guangzhou, China). Radioactivity measurements were performed using a γ-counter (CAPRAC-R, Capintec, Inc., Ramsey, NJ, USA).

Radiochemistry systhesis and quality control

[^{18}F]AlF-NOTA-Glc-Folate labeling was achieved via a one-step synthesizing approach based on Al^{18}F-chelation. Using the PET trace biomedical cyclotron (PET 800, General Electric, Boston, MA, USA), the n.c.a. $^{18}F^-$ was acquired. The QMA ion exchange column (Waters Corporation), pretreated with 5 mL of 0.5 M sodium bicarbonate solution and 10 mL of water, was used to trap $^{18}F^-$. After that, fluoride was eluted with 0.20 mL of 0.9% NaCl and 80 μLof the eluted $^{18}F^-$ was added to a mixture that included 50 μg of the precursor(NOTA-Glc-Folate), 280 μL of acetonitrile, 6 μL of 2 mM $AlCl_3$, and 5 μL of glacial acetic acid. After heating for 15 min at 105 °C, the mixture was cooled. Then the reaction liquid was diluted with 6 mL of water and moved to a SepPak C18 Plus cartridge (Waters Corporation), which was prepped with 5 mL of ethanol and 10 mL of water, then rinsed with 30 mL of water, and eluted with 1.5 mL of an ethanol/water mixture (1/1, v/v). The product was further diluted with saline for injection after passing through a 0.22 μm membrane filter into a sterile empty dose vial. Radio high-performance liquid chromatography (radio-HPLC) was used to evaluate the quality of the finished product.

The preparation process of the reference compound ([^{19}F]AlF-NOTA-Glc-Folate) was performed as follows. In brief, 2 μL of potassium fluoride (69.75 mM), 35 μL of $AlCl_3$ (2.0 mM), 6 μL of glacial acetic acid, 280 μL of acetonitrile and 100 μL of NOTA-Glc-Folate (697.5 μM) were mixed. The mixture was heated at 100 °C for 60 min. The reaction mixture was cooled to room temperature and then purified using a C18 cartridge.The C18 cartridge was washed with 30 mL of water. Finally, the Cl8 cartridge was eluted with 1.5 mL of ethanol. The purity of the eluted ethanol solution was detected separately by HPLC and ESI–MS.

The radiochemical purity of [^{18}F]AlF-NOTA-Glc-Folate was evaluated by an analytical radio-HPLC with a Kromasil 100-5 C18 column. A linear gradient was employed, starting from 95% A (0.1% trifluoroacetic acid in water) and 5% B (0.1% trifluoroacetic acid in acetonitrile), then transitioning to 55% A and 45% B at 2 min and reduced to 10% A at 14 min with a flow rate of 1.0 mL/min. The UV wavelength was monitored at 214 nm, while the radioactivity was quantified using a B-FC-3200 high-energy PMT detector manufactured by Bioscan Inc., located in Washington DC, USA.

Distribution coefficient

An aliquot (100 kBq) of [^{18}F]AlF-NOTA-Glc-Folate was added to a centrifuge tube containing a mixture of 3.0 mL of phosphate-buffered solution(PBS, pH 7.4) and an equal volume *n*-octanol. Following five minutes of vigorous vortexing at room temperature, the mixture underwent centrifugation for five minutes at 10,000 rpm. Then, three 100 μL samples from each phase were subjected to γ-counter for radioactivity detection.

Cell lines and the tumor models

FR-positive KB cells (purchased from Guangzhou Saiqiang Biotechnology Co., Ltd, China) and FR-negative A549 cells (purchased from Wuhan Biotechnology Co., Ltd, China) were utilized for cell-based experiments. KB cells were cultured in folate-deficient RPMI-1640 medium, while A549 cells were grown in DMEM media (Procell) at 37 °C with 5% carbon dioxide. 10% heat-inactivated fetal bovine serum (FBS) and 1% penicillin/streptomycin were added to both media.

The approval and execution of all animal research followed the guidelines of Southern Medical University's Nanfang Hospital's Institutional Animal Care and Use Committee(Application No: IACUC-LAC-20221031-003).

Female BALB/c nude mice (4–6 weeks old) were subcutaneously injected with KB cells or A549 cells in the right shoulder for micro-PET imaging and biodistribution experiments. The mouse was included in the in vivo studies as soon as the tumor reached a diameter of 5–10 mm.

In vitro and in vivo stability

For in vitro stability measurements, [^{18}F]AlF-NOTA-Glc-Folate(7.4 MBq) was added to PBS(200 µl) or FBS(200 µl) and incubated for 2 h at 37 °C. After filtration with a microporous filter membrane, an equal volume of the solution was subjected into radio-HPLC for in vitro stability studies.

For in vivo stability experiments, kunming mice were sacrificed 30 or 60 min after intravenous injection of the [^{18}F]AlF-NOTA-Glc-Folate (7.4–11.1 MBq per mouse). Subsequently, 500 µL of blood was drawn and mixed with an equivalent volume of acetonitrile. After five minutes of centrifugation at 10,000 rpm, 100 µL of the supernatant was utilized for a radio-HPLC analysis. Within 14 min, the eluted samples were manually collected at 30-s intervals and quantified with a γ-counter. Sample counts were plotted as the intensity (CPM) versus the fraction.

Cell studies

Cells were seeded onto 24-well plates one day before to reach a final confluence of about 80–90%. Before performing the experiments, a new 0.5 mL media without FBS replaced the old medium. After adding [^{18}F]AlF-NOTA-Glc-Folate, cells were incubated for 15, 30, 60, or 120 min at 37 °C.The medium was then removed, cells were washed twice with cold PBS (1.0 mL), and 1.0 mL 1 M NaOH lysate was added and collected. Radioactivity was determined using a γ-counter and reported as a percentage of the applied dosage (% ID/1 million cells). The blocking experiments were performed by including 2.3 µM folic acid. For the competitive binding assays, KB cells were incubated with [^{18}F]AlF-NOTA-Glc-Folate in the presence of 7 different concentrations (0, 10^{-11}, 10^{-10}, 10^{-9}, 10^{-8}, 10^{-7}, 10^{-6}, and 10^{-5} M) of the free folic acid or unlabeled precursor (NOTA-Glc-Folate) for 60 min at 37 °C [22]. Then, cells were washed twice with PBS in each experiment, lysed using 1 M NaOH and counted with a γ-counter. Using the uptake value of KB cells without added competitor as 100%, the half-maximum inhibitory concentration (IC_{50}) values of folic acid and precursor were obtained, which were determined utilizing a nonlinear regression approach to fit the data (implemented in Prism software).

Micro-PET imaging

After immobilization, mice with xenografted KB tumors or A549 tumors were placed in a micro-PET scanner (Siemens, Erlangen, Germany) in a prone position($n = 3$ per group). After the injection of [^{18}F]AlF-NOTA-Glc-Folate (5.5–11.1 MBq), dynamic micro-PET imaging was conducted within 120 min. Blocking experiments were performed by co-injecting 100 µg of folic acid in KB tumor-bearing mice. The images were reconstructed using a three-dimensional ordered-subset expectation maximum technique, and the outcome was expressed as a percentage of administered dosage per gram (%ID/g). The low-dose CT data, which was not enhanced, was used for attenuation correction. Decayed-corrected whole-body coronal images were obtained using Inevon Research Workplace 4.1 software, and tumors and important organs were manually delineated over the ROIs for data analysis.

Biodistribution studies

Mice bearing KB tumors or A549 tumors ($n = 3$ per group) were sacrificed 60 min after intravenous injection of [^{18}F]AlF-NOTA-Glc-Folate (740–1480 KBq/mouse). The blocking experiments were conducted in mice bearing KB tumors by co-injecting 100 µg of folic acid. Organs of interest, including spleen, blood, intestine, muscle, lung, heart, liver, gall bladder, stomach, uterus, ovary, kidney, and tumor were promptly excised and weighed. Using a γ-counter, radioactivity was measured and expressed as %ID/g.

Immunohistochemistry

Immunohistochemistry(IHC) staining experiments were performed on KB and A549 xenografted tumors to demonstrate FR expression. The tumor tissues were fixed, embedded in paraffin and then cut into 4 µm sections. IHC was performed according to a previously reported method [23]. The antibody for FR-α employed in this study was purchased from Guangzhou Wanshan Biotechnology Co., Ltd, China (Proteintech, 23355-1-AP).

Statistical analysis

The data were expressed as the mean ± standard deviation (SD). The statistical analyses were carried out using SPSS 22.0, a program developed and maintained by IBM Corp. in Armonk, NY, USA, to determine the significance of comparisons between two datasets. $P < 0.05$ were determined to statistically significant.

Results and discussion

Radiochemistry

The simplified radiolabeling process of [^{18}F]AlF-NOTA-Glc-Folate was shown in Fig. 1. The total duration of the synthesis process was within 30 min, and the non-decay corrected radiochemical yield of [^{18}F]AlF-NOTA-Glc-Folate was 22.5 ± 1.8% (n = 6). The radiochemical purity of [^{18}F]AlF-NOTA-Glc-Folate was higher than 99% based on radioactivity measurements without undergoing HPLC purification, and the apparent molar radioactivity of [^{18}F]AlF-NOTA-Glc-Folate was 12–30 GBq/μmol. In contrast to the previously reported aluminum fluoride labeling methods [14, 16], the labeling method used in this paper exhibited a higher radiochemical yield with radiochemical purity.

Partition coefficient and stability

Due to the introduction of hydrophilic group(-Glc), the n-octanol/PBS distribution coefficients (logD) values of [^{18}F]AlF-NOTA-Glc-Folate was − 3.64 ± 0.55 (n = 4), indicating a high hydrophilicity.

In vitro stability results showed [^{18}F]AlF-NOTA-Glc-Folate demonstrated remarkable stability in PBS and FBS with no degradation (radiochemical purity > 98%). Additionally, the in vivo stability studies of [^{18}F]AlF-NOTA-Glc-Folate were assessed using mouse blood supernatant, with the recovery rate of the radiolabeled tracer being 63.29 ± 1.59%. In 30 min, the main peak of [^{18}F]AlF-NOTA-Glc-Folate constituted more than 95%, but by 60 min, it had reduced to 88% (Fig. 2), probably because it was internalized into cells after binding to FR and was involved in cellular metabolic activity [24].

Cellular studies

Cellular uptake studies were conducted using KB and A549 cells to examine the binding specificity of [^{18}F]AlF-NOTA-Glc-Folate to FR-α (Fig. 3a). Within 120 min, the uptake of KB cells significantly exceeded that of A549 cells, increasing slightly over time. Furthermore, after incubation with excessive folic acid, the uptake of [^{18}F]AlF-NOTA-Glc-Folate on KB cells was significantly reduced (2.6 ± 0.1 vs. 0.2 ± 0.1, p < 0.01) (Fig. 3b), suggesting that [^{18}F]AlF-NOTA-Glc-Folate was uptake with specificity to FR. To ascertain the affinity of [^{18}F]AlF-NOTA-Glc-Folate for FR, we subsequently conducted competition binding assays (Fig. 3c). As we are exspected, NOTA-Glc-Folate (IC_{50} = 21.92 ± 0.87 nM) was about sevenfold higher than folic acid (IC_{50} = 2.95 ± 0.53 nM) in FR-expressing KB

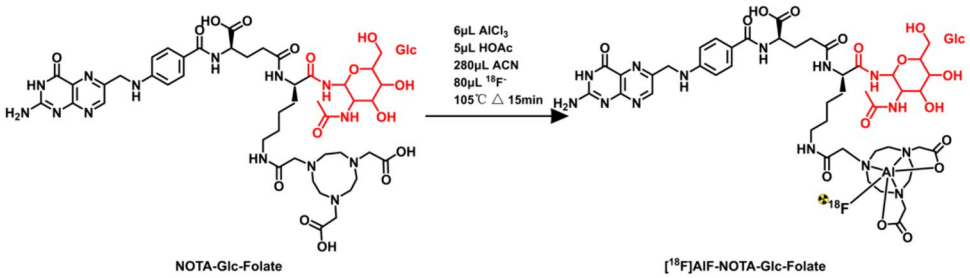

Fig. 1 Radiochemical synthesis process of the [^{18}F]AlF-NOTA-Glc-Folate. HOAc: acetic acid, ACN: acetonitrile

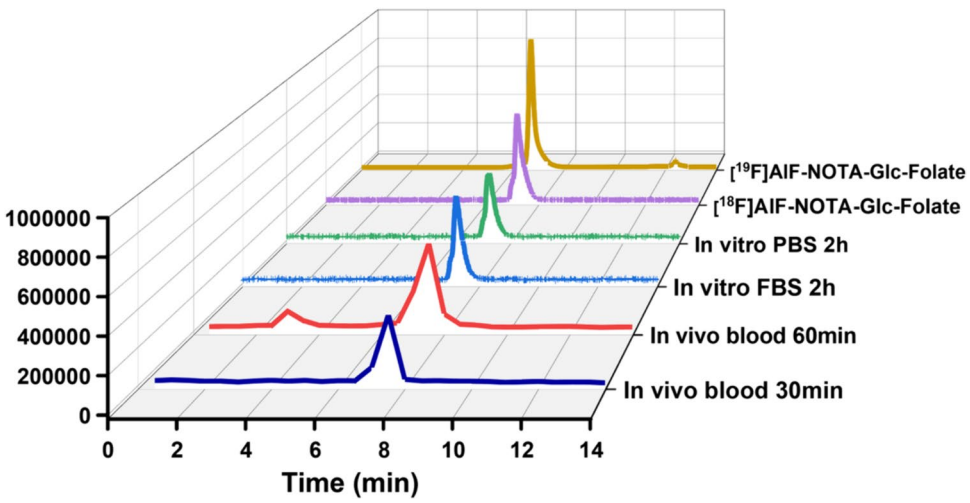

Fig. 2 Representative HPLC profiles for quality control, in vitro and in vivo stabilities of [^{18}F]AlF-NOTA-Glc-Folate, as well as the UV chromatography of the reference compound [^{19}F]AlF-NOTA-Glc-Folate

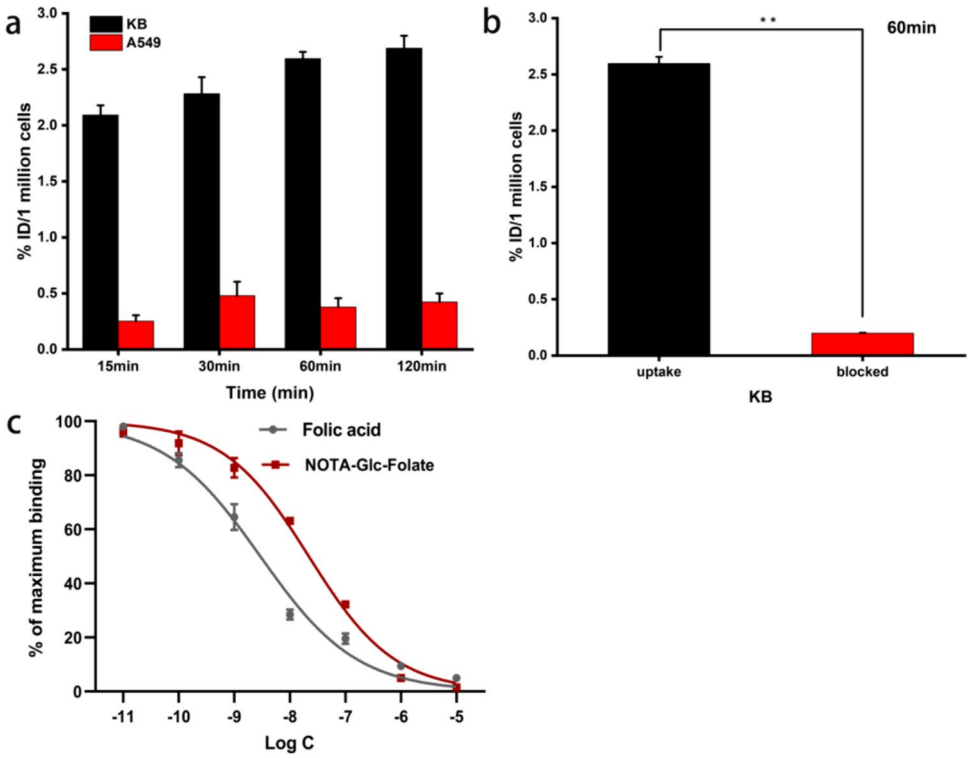

Fig. 3 **a** Cell uptake of [^{18}F]AlF-NOTA-Glc-Folate in KB cells or A549 cells after incubation for 15–120 min. **b** Uptake of [^{18}F]AlF-NOTA-Glc-Folate in KB cells after incubation for 60 min, with and without free folic acid as a competitor. **c** Competitive binding of [^{18}F]AlF-NOTA-Glc-Folate ($IC_{50}=21.92\pm0.87$ nM) and folic acid ($IC_{50}=2.95\pm0.53$ nM) on KB cells ($n=4$). $^{**}p<0.01$

cells. The results suggested that the receptor binding affinity of folic acid was not considerably affected by structural modification to the γ-carboxylic acid of the glutamic acid segment [25, 26].

Micro-PET imaging

Using the ^{18}F-labeled folic acid derivative [^{18}F]AlF-NOTA-Glc-Folate, dynamic micro-PET imaging experiments were performed in mice bearing KB tumors or A549 tumors. The representative maximum intensity projection (MIP) images and time-activity curves of [^{18}F]AlF-NOTA-Glc-Folate showed low uptake and rapid clearance in most organs of KB or A549 tumor-bearing mice within 120 min p.i. (Fig. 4). The micro-PET imaging with [^{18}F]AlF-NOTA-Glc-Folate revealed an appropriate uptake of KB tumours(1.8 ± 0.3% ID/g) at 60 min p.i., and the tumors were apparent shortly after injection (15 min p.i.). The continuously improving contrast with liver during the scanning period; meanwhile, the ratios of tumor-to-muscle peaked at 60 min p.i. (Fig. 4f). Attributed to the physiological expression of FR-α, [^{18}F]AlF-NOTA-Glc-Folate showed a high uptake and excellent retention in the kidneys (23.4 ± 2.3% ID/g at 60 min p.i.), however, it showed a low uptake in other normal organs, indicating that the tracer was primarily excreted through the kidneys.

Next, a comparison of tumor uptake and blocking investigations was performed in mice bearing KB tumors with [^{18}F]AlF-NOTA-Glc-Folate (Fig. 4e). When free folic acid was co-injected, the uptake of [^{18}F]AlF-NOTA-Glc-Folate in KB tumors (from 1.8 ± 0.3 to 0.5 ± 0.1% ID/g, $p<0.01$) and kidneys (from 22.2 ± 3.0 to 1.7 ± 0.2% ID/g, $p<0.01$) was significantly reduced at 60 min p.i., indicating FR-specific targeting.

Biodistribution studies

To evaluate the FR' binding abilities of [^{18}F]AlF-NOTA-Glc-Folate in vivo, biodistribution experiments were carried out in mice bearing KB or A549 tumors at 60 min p.i. (Fig. 5). Consistent with micro-PET imaging results, biodistribution experiments showed that the uptake of [^{18}F]AlF-NOTA-Glc-Folate was concentrated primarily in KB tumors(1.8 ± 0.2% ID/g) and kidneys(22.2 ± 3.0% ID/g). Co-injection of excess folic acid could obviously reduce its uptake and retention in tumors(from 1.8 ± 0.2 to 0.2 ± 0.1% ID/g at 60 min p.i., $p<0.01$) and kidneys(from 22.2 ± 3.0 to 1.2 ± 0.3% ID/g at 60 min p.i., $p<0.01$) suggested the accumulation of [^{18}F]AlF-NOTA-Glc-Folate was mediated by FR. Mice bearing A549 tumors were used as control models, and the uptake was approximately sixfold lower(0.3 ± 0.1% ID/g, $p<0.01$). As we are expected, the uptake of [^{18}F]AlF-NOTA-Glc-Folate was significantly reduced in the kidneys and liver (22.2 ± 3.0 and 0.3 ± 0.1% ID/g at 60 min p.i.) compared to the known tracer [^{18}F]AlF-NOTA-Folate (78.6 ± 5.1 and 5.3 ± 0.5% ID/g at 90 min p.i., $p<0.01$) [16] and [^{18}F]

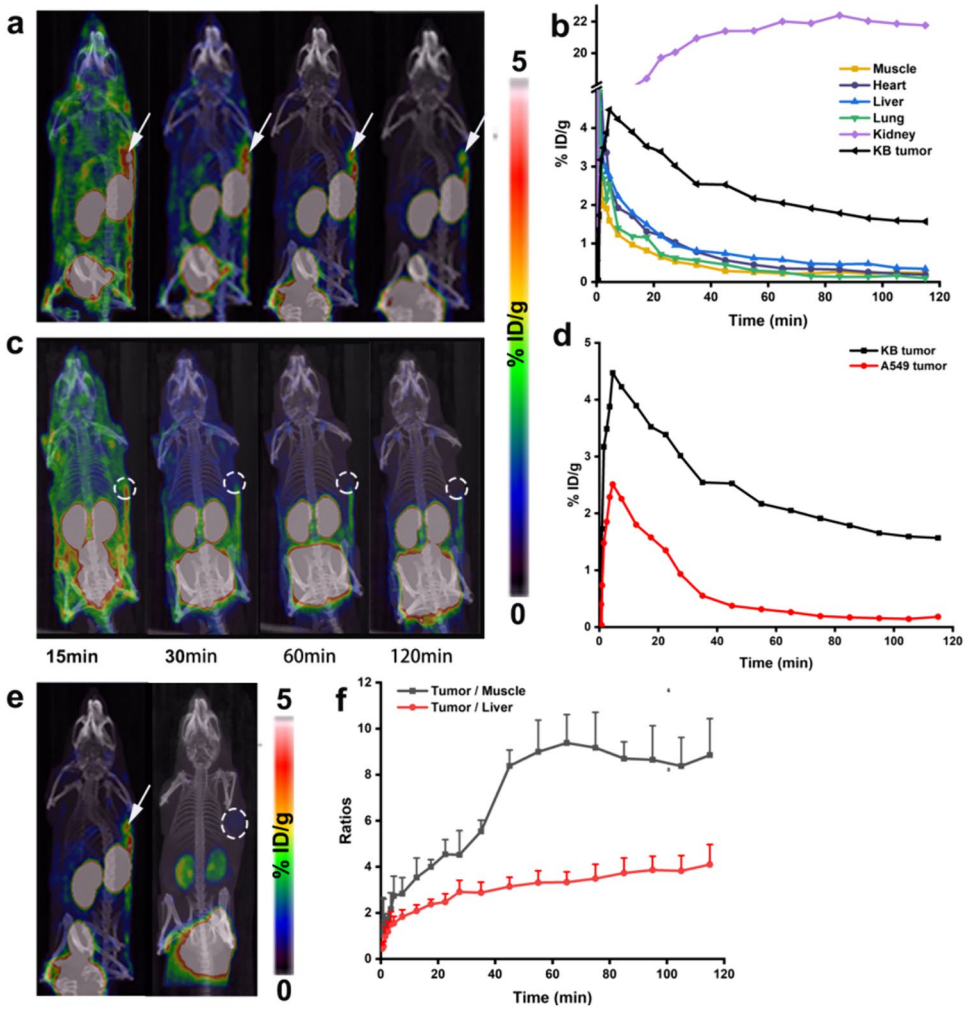

Fig. 4 Representative micro-PET images and time-activity curves. **a** MIP images of [^{18}F]AlF-NOTA-Glc-Folate in mice bearing KB tumors at 15, 30, 60, and 120 min p.i. ($n=3$). **b** Time-activity curves of tumor and major organs after the intravenous injection of [^{18}F]AlF-NOTA-Glc-Folate in KB tumor-bearing mice. **c** MIP images of [^{18}F]AlF-NOTA-Glc-Folate in mice bearing A549 tumors at 15, 30, 60, and 120 min p.i. ($n=3$). **d** Time-activity curves of KB and A549 tumors after the intravenous injection of [^{18}F]AlF-NOTA-Glc-Folate. **e** MIP images of [^{18}F]AlF-NOTA-Glc-Folate in KB tumor-bearing mice at 60 min p.i., with or without the 100ug folic acid as a competitor ($n=3$). **f** The ratios of tumor-to-muscle/liver for 120 min p.i. of [^{18}F]AlF-NOTA-Glc-Folate in mice bearing KB tumors. Arrows and circles represent the locations of the tumors

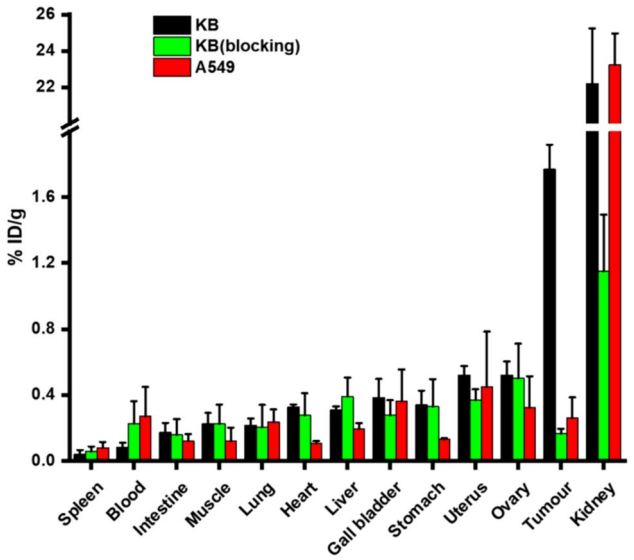

Fig. 5 Biodistribution results of [^{18}F]AlF-NOTA-Glc-Folate in mice with KB tumors or A549 tumors at 60 min p.i., with or without 100 μg folic acid. All data were expressed as mean ± SD ($n=3$)

AlF-NOTA-PEG$_{12}$-Folate (55.2 ± 7.4 and 1.6 ± 0.3% ID/g at 90 min p.i., $p<0.01$) [14]. Additionally, the uptake of [^{18}F]AlF-NOTA-Glc-Folate in muscle, heart, spleen and lung showed varying degrees of reduction, indicating the Glc linker helped improve the in vivo clearance behavior of a radiotracer [17–21]. Regrettably, the tumor uptake of [^{18}F]AlF-NOTA-Glc-Folate (1.8 ± 0.2% ID/g, 60 min p.i.) was also significantly reduced in comparison with [^{18}F]AlF-NOTA-Folate (10.9 ± 2.7% ID/g, 90 min p.i.) and [^{18}F]AlF-NOTA-PEG$_{12}$-Folate (9.2 ± 0.6% ID/g, 90 min p.i.) [14, 16]. Nevertheless, relatively low uptake in the kidney and hepatobiliary systems, as well as low uptake and rapid clearance in most normal organs, showed that [^{18}F]AlF-NOTA-Folate seemed to be a potential radiotracer for PET imaging of FR-positive tumors.

Immunohistochemistry

The tumor tissue samples from KB and A549 tumor-bearing mice were analyzed by immunohistochemistry to ascertain the protein expression levels of FR-α. The

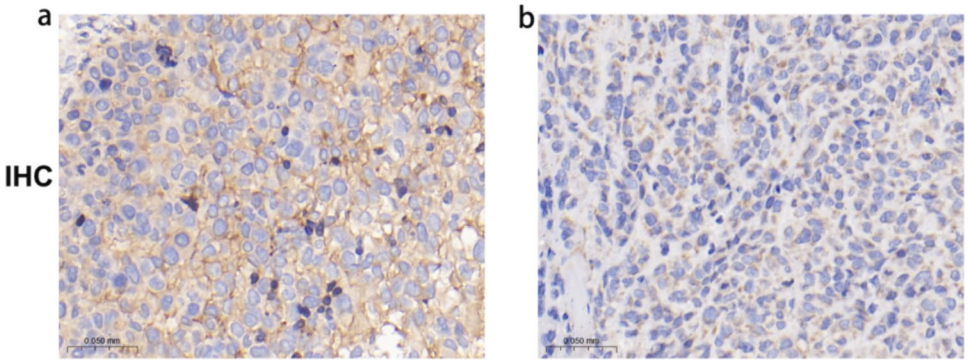

Fig. 6 Immunohistochemistry staining of KB tumor (**a**) and A549 tumor (**b**) section. Tissue images were shown in magnification 40×

cellular membranes of KB tumor showed a strong and noticeable brown stain, indicating FR-α overexpression (Fig. 6a). The A549 tumor cell membranes showed a weak brown stain, indicating a weak expression of FR-α (Fig. 6b).

Conclusion

A novel folic acid derivative PET tracer ([^{18}F]AlF-NOTA-Glc-Folate) with high radiochemical yield and purity was designed and synthesized in a simple and efficient one-step reaction for FR-positive tumors imaging. Experiments carried out in vitro demonstrated that [^{18}F]AlF-NOTA-Glc-Folate had great stability, and selective targeting to the FR. In vivo studies exhibited that [^{18}F]AlF-NOTA-Glc-Folate specifically bound to FR-positive tumors, and significantly reduced the uptake and retention in normal organs, particularly in the kidney and liver. Taking together, [^{18}F]AlF-NOTA-Glc-Folate, with its simple synthesis procedure, high radiochemical yield and purity, proper tumor uptake, and favorable pharmacokinetic properties, holds promise for noninvasive imaging of tumors with FR expression.

Acknowledgements This study is funded by the National Natural Science Foundation of China (grants 82371996, 91949121), the National Key Research and Development Program (2022YFC2403803), Guangdong Basic and Applied Basic Research Foundation (grants 2022A1515010072, 2020A1515011399), Guangzhou Science and Technology Plan (2023B03J0529), Medical Products Administration of Guangdong Province (grants 2021ZDB02, Drug Supervision and Administration Division 1 (2022)), and Nanfang Hospital Talent Introduction Foundation of Southern Medical University (No. 123456).

Author contribution's Haoran Liang and Zihao Chen contribute equally to the work. Conception and study design: Ganghua Tang, Haoran Liang, Zihao Chen, and Shuqi Ren; experimental execution: Haoran Liang, Zihao Chen, and Shuqi Ren; data analysis: Haoran Liang and Zihao Chen; administrative, technical, or material support: Ganghua Tang, Haoran Liang, and Chunwei Mo; writing—original draft preparation: Haoran Liang; writing—review and editing: Haoran Liang and Ganghua Tang; funding acquisition: Ganghua Tang. All authors have reviewed and approved the final manuscript.

Availability of data and material The datasets used or analysed during the current study are available from the corresponding author on reasonable request.

Declarations

Conflict of interest All authors declare that they have no conficts of interest.

Ethical approval All animal studies were performed according to a protocol approved by the Southern Medical University Nanfang Hospital Animal Care and Use Committee (Application No: IACUC-LAC-20221031-003).

Consent for publication All authors consent to the publication of this manuscript.

References

1. Boss SD, Ametamey SM (2020) Development of folate receptor-targeted PET radiopharmaceuticals for tumor imaging—a bench-to-bedside journey. Cancers (Basel) 12:1508
2. Parker N, Turk MJ, Westrick E, Lewis JD, Low PS, Leamon CP (2005) Folate receptor expression in carcinomas and normal tissues determined by a quantitative radioligand binding assay. Anal Biochem 338:284–293
3. Low PS, Kularatne SA (2009) Folate-targeted therapeutic and imaging agents for cancer. Curr Opin Chem Biol 13:256–262
4. Mathias CJ, Lewis MR, Reichert DE et al (2003) Preparation of ^{66}Ga- and ^{68}Ga-labeled Ga(III)-deferoxamine-folate as potential folate-receptor-targeted PET radiopharmaceuticals. Nucl Med Biol 30:725–731
5. Fani M, Wang X, Nicolas G et al (2010) Development of new folate-based PET radiotracers: preclinical evaluation of ^{68}Ga-DOTA-folate conjugates. Eur J Nucl Med Mol Imaging 38:108–119
6. Brand C, Longo VA, Groaning M, Weber WA, Reiner T (2017) Development of a new folate-derived Ga-68-based PET imaging agent. Mol Imaging Biol 19:754–761
7. Müller C, Vlahov IR, Santhapuram HK, Leamon CP, Schibli R (2010) Tumor targeting using ^{67}Ga-DOTA-Bz-folate investigations of methods to improve the tissue distribution of radiofolates. Nucl Med Biol 38:715–723
8. Gnesin S, Müller J, Burger IA et al (2020) Radiation dosimetry of [^{18}F]-AzaFol: a first in-human use of a folate receptor PET tracer. EJNMMI Res 10:32

9. Siegel BA, Dehdashti F, Mutch DG et al (2003) Evaluation of ^{111}In-DTPA-folate as a receptor-targeted diagnostic agent for ovarian cancer: initial clinical results. J Nucl Med 44:700–707
10. Fisher RE, Siegel BA, Edell SL et al (2008) Exploratory study of ^{99m}Tc-EC20 imaging for identifying patients with folate receptor-positive solid tumors. J Nucl Med 49:899–906
11. Boss SD, Müller C, Siwowska K et al (2018) Reduced ^{18}F-folate conjugates as a new class of PET tracers for folate receptor imaging. Bioconjug Chem 29:1119–1130
12. Shi X, Xu P, Cao C, Cheng Z, Tian J, Hu Z (2022) PET/NIR-II fuorescence imaging and image-guided surgery of glioblastoma using a folate receptor α-targeted dual-modal nanoprobe. Eur J Nucl Med Mol Imaging 49:4325–4337
13. Feng J, Zhang X, Ruan Q, Jiang Y, Zhang J (2021) Preparation and evaluation of novel folate isonitrile ^{99m}Tc complexes as potential tumor imaging agents to target folate receptors. Molecules 26:4552
14. Chen Q, Meng X, McQuade P et al (2017) Folate-PEG-NOTA-Al^{18}F: a new folate based radiotracer for PET imaging of folate receptor-positive tumors. Mol Pharm 14:4353–4361
15. Benešová M, Guzik P, Deberle LM, Busslinger SD, Landolt T, Schibli R, Müller C (2022) Design and evaluation of novel albumin-binding folate radioconjugates: systematic approach of varying the linker entities. Mol Pharm 19:963–973
16. Chen Q, Meng X, McQuade P et al (2016) Synthesis and preclinical evaluation of folate-NOTA-Al^{18}F for PET imaging of folate receptor-positive tumors. Mol Pharm 13:1520–1527
17. Huang J, Fu L, Zhang X et al (2023) Noninvasive imaging of FAP expression using positron emission tomography: a comparative evaluation of a [^{18}F]-labeled glyopeptide-containing FAPI with [^{18}F]FAPI-42. Eur J Nucl Med Mol Imaging 50:3363–3374
18. Schottelius M, Wester HJ, Reubi JC, Senekowitsch-Schmidtke R, Schwaiger M (2002) Improvement of pharmacokinetics of radioiodinated Tyr(3)-octreotide by conjugation with carbohydrates. Bioconjug Chem 13:1021–1030
19. Potemkin R, Strauch B, Kuwert T, Prante O, Maschauer S (2020) Development of ^{18}F-fluoroglycosylated PSMA-ligands with improved renal clearance behavior. Mol Pharm 17:933–943
20. Moradi SV, Hussein WM, Varamini P, Simerska P, Toth I (2016) Glycosylation, an effective synthetic strategy to improve the bioavailability of therapeutic peptides. Chem Sci 7:2492–2500
21. Maschauer S, Einsiedel J, Haubner R et al (2010) Labeling and glycosylation of peptides using click chemistry: a general approach to ^{18}F-glycopeptides as effective imaging probes for positron emission tomography. Angew Chem Int Ed Engl 49:976–979
22. Fani M, Wang X, Nicolas G et al (2011) Development of new folate-based PET radiotracers: preclinical evaluation of ^{68}Ga-DOTA-folate conjugates. Eur J Nucl Med Mol Imaging 38:108–119
23. Sun P, Han Y, Hu K et al (2022) Synthesis and biological evaluation of Al[^{18}F]-NOTA-IPB-PDL1P as a molecular probe for PET imaging of PD-L1 positive tumors. Bioorg Chem 122:105682
24. Sabharanjak S, Mayor S (2004) Folate receptor endocytosis and trafficking. Adv Drug Deliv Rev 56:1099–1109
25. Das S, Sakhare N, Kumar D et al (2023) Design, characterization and evaluation of a new ^{99m}Tc-labeled folate derivative with affinity towards folate receptor. Bioorg Med Chem Lett 86:129240
26. Chen C, Ke J, Zhou XE (2013) Structural basis for molecular recognition of folic acid by folate receptors. Nature 500:486–489